CENTRE FOR
FINANCIAL RISK
*Faculty of Business and Economics*

MACQUARIE University

# A Bayesian Real Options Model for Adaptation to Catastrophic Risk under Climate Change Uncertainty

WORKING PAPER 16-04

Chi Truong, Stefan Trueck and Tak Kuen Siu

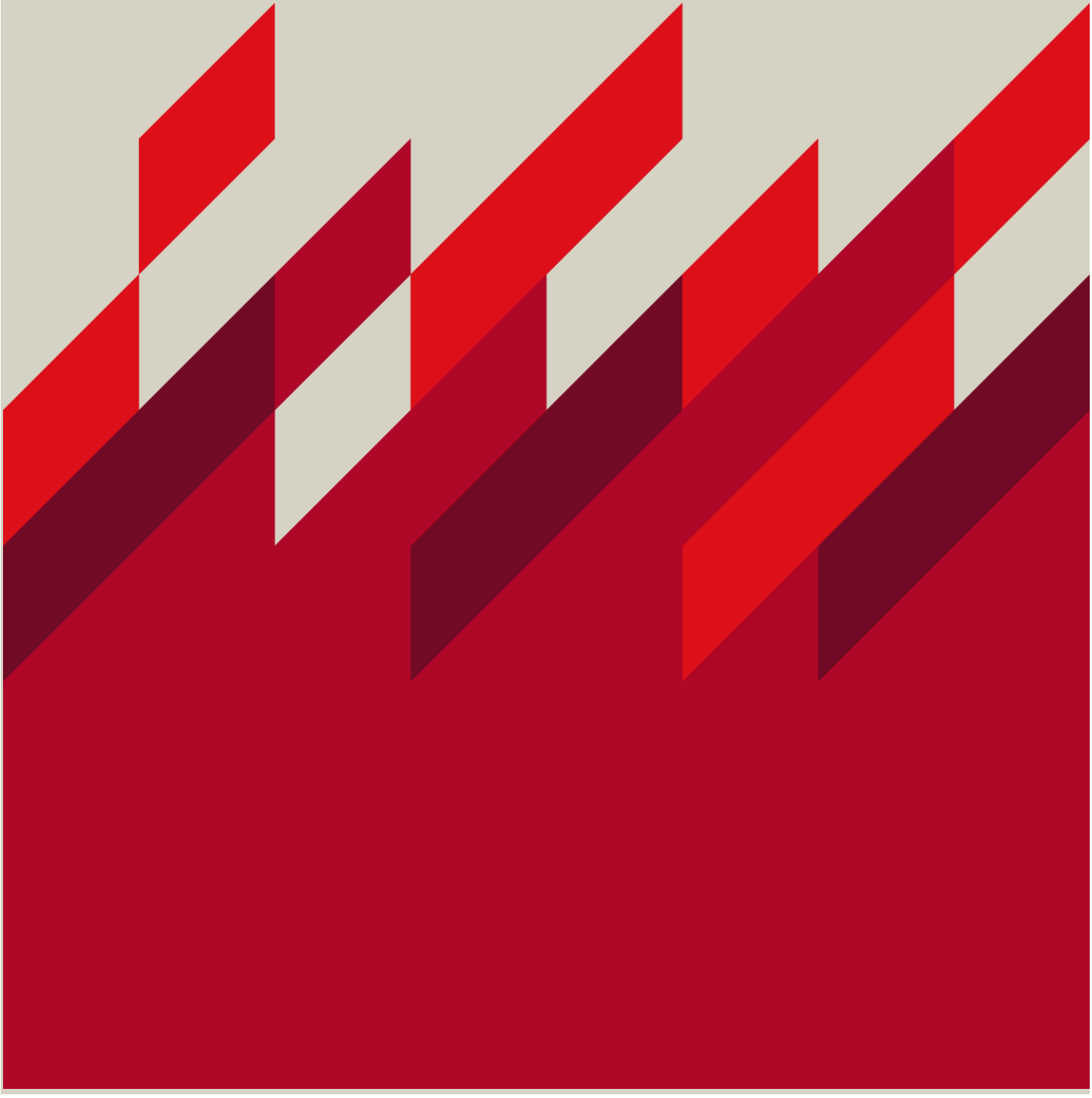

# A Bayesian Real Options Model for Adaptation to Catastrophic Risk under Climate Change Uncertainty

Chi Truong[1], Stefan Trück[1], Tak Kuen Siu[1]

[a]*Faculty of Business and Economics, Macquarie University, NSW, Australia, 2109*

**Abstract**

We present a novel framework for the valuation of investments to mitigate catastrophic risk of climate impacted hazards. Our model incorporates the impact of uncertainty and continuous Bayesian information updating on investment decisions. We show that the model is relevant even when the time required to resolve uncertainty is indefinite. The model is applied to bushfire risk management in a local area. Our findings suggest that investment based on the net present value (NPV) rule that ignores the value of the investment option results in significant losses. Sensitivity analysis results suggest that the loss is large when the investment cost is high, when the uncertainty resolution is slow, or when the probability belief in climate change is low.

*Keywords:* Climate Change Adaptation, Real Option Analysis, Partial Observation, Catastrophic Risk, Bayesian Models, Decision-Making under Uncertainty
*JEL Codes*: D81, Q54, C02, C11, H54.

*Email addresses:* chi.truong@mq.edu.au (Chi Truong), stefan.trueck@mq.edu.au (Stefan Trück), Ken.Siu@mq.edu.au (Tak Kuen Siu)

## 1. Introduction

Significant developments in real options theory over the last two decades have made real options a popular tool for the valuation of irreversible investments. In stochastic environments, where project values are uncertain and investment is irreversible, the rational decision to invest is analogous to the optimal exercise of an American option. Thus, an investment option can be valued and the option should be relinquished only when the value of the project is sufficiently high. Real options theory has been used to explain firms' investment behaviour that cannot be explained by the discounted cash flow theory based on net present values (NPV) (Quigg, 1993; Carey and Zilberman, 2002) and has been applied in various fields of research, see, e.g., Dixit and Pindyck (1994); Schwartz and Trigeorgis (2004) for an overview.

Despite the appeal of real options theory in guiding investment under uncertainty, few applications exist in the area of climate change adaptation, especially in the valuation of projects that may mitigate catastrophic risks. This seems surprising, since investment projects in this area, e.g. flood dykes or dams, often last for decades and investment is therefore difficult, if not impossible, to reverse. The demand for accurate valuation of such adaptation projects is certainly high, given the enormous investment costs. In addition, uncertainty induced by climate change is immense and the most important impact of climate change is often thought to be through catastrophes (Van Aalst, 2006). The importance of 'real options thinking' in the field of climate change has been recognised by Gollier and Treich (2003).

The main difficulty in applying existing real options models to climate change adaptation is that typically in these models, the underlying probability law that describes uncertainty in investment payoffs is assumed to be known (Dixit and Pindyck, 1994). Therefore, in most of the standard real options models, only the investment payoff is uncertain and varies stochastically over time. While this assumption is reasonable in a stationary environment, it may not be suitable in the context of climate change adaptation where the climate system is known to be changing[1], but the extent of the change is uncertain.

[1] As shown in Hartmann et al. (2014), observed data on global mean temperature indicates an increase

Appropriate models need to take into account uncertainty about parameters in stochastic models, which is usually called 'deep uncertainty', and how that uncertainty resolves over time as more observations on climate change impacts become available. In the absence of a scientifically rigorous model, climate change adaptation studies often revert to discounted cashflow theory and use the NPV rule to make investment decisions (Kirshen et al., 2008a,b; Michael, 2007; Symes et al., 2009; West et al., 2001; Brouwer and van Ek, 2004; Waters et al., 2003; Zhu et al., 2007; Bouwer et al., 2010; Mathew et al., 2012). In a recent study, Li et al. (In press) use Bayesian approaches for analyzing catastrophic risks resulting from earthquakes. They, however, focus on the use of Extreme Value Theory coupled with a Markov chain Monte Carlo (MCMC) approach to estimate catastrophic risk, which is not the same as the focus of the current paper.

In this paper, we examine an optimal investment problem at a regional level to reduce the risk of catastrophes such as bushfires, flooding and storm surges. These are important catastrophes that result in large costs to the insurance industry. For example, insurance cost in Australia over the period 1990-2012 for bushfires, flooding and storm surges are \$1.8, \$3.06, and \$0.86 billion, respectively (Insurance Council of Australia, 2016). In a hotter and therefore more energetic climate system, these catastrophes are predicted to occur even more frequently (Solomon, 2007). For Australia, recent studies suggest that Queensland will observe more floods and storm surges, while in the southeastern Australia, a higher number of bushfires is predicted to occur (Garnaut, 2011; Murphy and Timbal, 2008). These trends seem to be already present in the records of Australian insurance costs (Figure 1). The costs of insuring bushfire, flooding and storm surge losses appear to have grown exponentially over the last two decades, from a total of \$0.47 billion in the 1990s to \$5.2 billion in the 2000s.

of 0.075°C per decade if a linear model is estimated for the period 1901-2012, and 0.107°C per decade if a piece-wise linear model is used. For Australia, data over the period 1957-1996 indicates that occurrences of warm temperature extreme events have increased while the number of extremely cool temperature events has decreased (Collins et al., 2000).

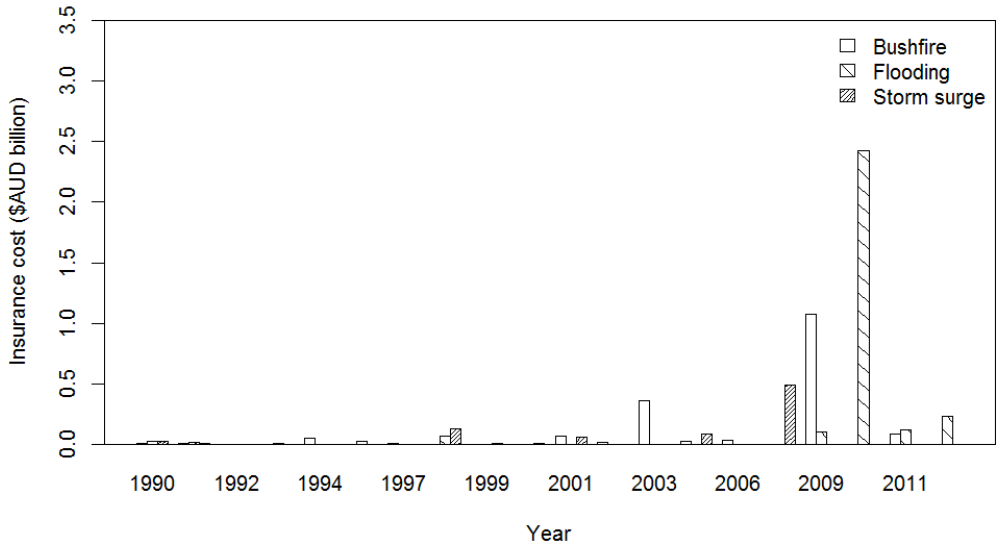


Figure 1: Annual insurance cost of bushfires, flooding and storm surges in Australia over period 1990-2012. Data are sourced from Insurance Council of Australia (2016).

As a result of more frequent and possibly more severe catastrophic losses, the payoffs of risk reduction projects grow over time. The growth rate of the payoffs is, however, highly uncertain due to the uncertainty in climate change predictions and in the mechanisms used to downscale global climate change estimates to regional scales. Using different climate models and different emission scenarios, one can obtain quite different predictions for the frequency and severity of climate impacted hazards. A decision maker can form an initial probability belief on the growth of investment payoff based on the predictions from climate models and update this belief when more observations on the local climate, and therefore catastrophic risk, are available. Studies in climate change, see, e.g., Kelly and Kolstad (1999); Karp and Zhang (2006), however, found that initial beliefs based on climate models often reflect immense uncertainty and the uncertainty takes a long time to resolve. In the case of climate change adaptation, this means that we may never know the true growth rate of investment payoffs. An important question is whether it is still worthwhile to defer investment rather than investing immediately given a positive NPV, while this uncertainty is never resolved. Furthermore, in implementing an investment model at the regional level, it is often found that few observations of catastrophic events are available and the question of how to overcome data scarcity also needs to be addressed.

We contribute to the literature by introducing a real options framework for the valuation of catastrophic risk mitigation projects that allows for continuous Bayesian updating of information. Our framework is built upon recent work in the field of investment under incomplete information (Décamps et al., 2005; Klein, 2009) but quite significantly extends these studies to allow for a more general payoff structure: while Décamps et al. (2005) and Klein (2009) examine so-called 'front-loaded' projects, i.e. projects where all payoffs are obtained immediately upon investment, we investigate the investment decision for a 'back-loaded' project where payoffs are spread across the entire lifetime of the project which is assumed to be indefinite. This seems an important extension from the practical perspective, since in practice most investment projects for catastrophe prevention or adaptation to climatic change last for a long time and payoffs are typically obtained while the projects are still in place.

We find that investment behaviour for back-loaded projects can be significantly different from that for front-loaded projects. In particular, the optimal investment boundary in the payoff-belief state space is found to be non-increasing rather than non-decreasing as found by Décamps et al. (2005) and Klein (2009). This means that the more pessimistic the decision maker is about the growth rate of the payoff flow, the longer she delays investment. This result is shown to hold in a special case where the logarithm of investment payoff follows a random walk process without drift and in the conducted empirical study.

We also analyse the expected time to learn about the growth rate of payoffs from the investment and the expected time to investment that are of great interest in climate change adaptation (Chao and Hobbs, 1997; Kelly and Kolstad, 1999). In contrast to the usual perception, see, e.g. Grenadier and Malenko (2010), we show that in a modelling framework with an unknown growth rate, uncertainty may remain unresolved forever and one may never know the true growth rate. This is evidenced in our empirical example and may well occur for other climate change adaptation problems. We show that the expected time to investment may also be infinite, but it is still important to use the real options framework to capture the positive value generated by volatile investment payoffs.

A nice feature of the developed model is that when the logarithm of the investment pay-

off follows a random walk process without drift, we can calculate the exact value of the investment option using a closed form formula. When this is not the case, the model can be solved using standard numerical techniques such as, e.g. binomial lattice or finite difference methods. We illustrate the application of the model for the case of bushfire risk management at the local level. We use a Poisson panel data model to estimate the loss frequency and apply quantile regression to estimate the distribution for the severity of losses. Both of these econometric models utilize broad databases to overcome the rare-event data shortage problem. Quantile regression also takes account of heavy tails inherent in catastrophic losses and allows to investigate factors driving extreme losses separately from those that affect average losses. This flexibility proves valuable in particular for exploring the complex relationship between climate change, adaptation and catastrophic loss events.

The remainder of the paper is organized as follows. Section 2 outlines and analyzes the developed modeling framework. Section 3 provides an application of the framework in a case study, using catastrophic risks from bushfires as an empirical example. The final Section 4 concludes.

## 2. Modeling framework

### *2.1. Frequency and Severity of Climate Impacted Hazards*

In the following, we model the cumulative loss $S_t$ over a period $(0, t]$ as a compound Poisson process

$$S_t = \sum_{n=1}^{N_t} X_n, \tag{2.1}$$

where $N_t$ is the number of catastrophic events that occur during period $(0, t]$ and $X_n$ is the loss caused by the $n^{th}$ event. It is assumed that $X_n$, $n = 1, 2, \cdots$, are independent and identically distributed random variables, which are also independent of $N_t$. The loss severity has an expected value $\beta$ and the number of catastrophic events, $N_t$, follows a conditional Poisson process that has a stochastic intensity $\Lambda_t$. The process $\{\Lambda_t\}$ is assumed to follow a geometric Brownian motion

$$d\Lambda_t/\Lambda_t = \mu dt + \sigma dB_t,$$

where $\{B_t\}$ is a standard Brownian motion defined on a given complete probability space $(\Omega, \mathcal{F}, P)$. The drift $\mu$ is a random variable on $(\Omega, \mathcal{F}, P)$ taking a value in the state space $\{\mu_H, \mu_L\}$ [2]. The volatility of the Poisson intensity process $\sigma$ is assumed to be a positive constant for simplicity. The positivity of $\Lambda_t$ follows since the intensity process $\{\Lambda_t\}$ is governed by a geometric Brownian motion[3].

The decision maker has an initial belief $p_0$ that the growth rate is $\mu_H$ and updates her belief as information about the Poisson intensity emerges, using the Bayes' rule, so that the information updating is rational. The $\sigma$-field generated by the process $\{\Lambda_t\}$ up to and including time $t$ augmented by all $P$-null subsets of $\mathcal{F}$ is denoted by $\mathscr{F}_t$ and the posterior probability of event $\mu = \mu_H$ at time $t$ is denoted by $P_t$, i.e. $P_t = P[\mu = \mu_H | \mathscr{F}_t]$, with the initial condition $P_0 = p_0$. Upon applying Bayes' rule, the posterior probability $P_t$ can be expressed as

$$P_t = \left[1 + \frac{1-p_0}{p_0}\left(\exp\left((\ln\Lambda_t - \ln\Lambda_0 - \frac{\mu_H + \mu_L - \sigma^2}{2}t)\right)\right)^{-\omega/\sigma}\right]^{-1}, \qquad (2.2)$$

where $\omega = \frac{\mu_H - \mu_L}{\sigma}$ is interpreted as the signal to noise ratio. It can be checked that $P_t \in (0,1)$. Equation (2.2) implies that $P_t$ is revised upwards (downwards) whenever $\ln\Lambda_t$ is higher (lower) than its expected value, $\ln\Lambda_0 + \frac{\mu_H + \mu_L - \sigma^2}{2}t$, that is obtained when $\mu$ takes the average level, $\mu = \frac{\mu_H + \mu_L}{2}$. The extent of revision is proportional to the difference between $\ln\Lambda_t$ and its expected value, the level of uncertainty $\mu_H - \mu_L$, and is inversely proportional to the noise level measured by $\sigma$.

We can describe the dynamics of the posterior belief $P_t$ by using another Brownian motion

[2] In general, one may consider the situation where $\mu$ can take any real values. In particular, if $\mu$ has a prior distribution as a normal distribution, we may end up with a conjugate-prior situation and the posterior estimate of $\mu$ can be derived by solving a heat equation, as in, for example, Karatzas and Zhao (2001) and Zhang et al. (2012). However, to illustrate the key idea of the present modeling framework and to simplify our discussion, we consider the simpler situation where $\mu$ takes a value in $\{\mu_H, \mu_L\}$

[3] Note that in a more general setting, one may also consider the situation where the drift of the Poisson intensity process is modulated by a hidden Markov chain. However, under such a setting, filtering theory for hidden Markov models would be required to discuss the problem. This may perhaps represent a potential topic for future research.

$\{\bar{B}_t\}$ that is adapted to the filtration $\{\mathscr{F}_t\}$ [4],

$$\bar{B}_t \equiv \sigma^{-1}\left(\ln \Lambda_t - \ln \Lambda_0 - \int_0^t E(\mu|\mathscr{F}_s)ds + \frac{1}{2}\sigma^2 t\right). \tag{2.3}$$

As discussed in Liptser and Shiryaev (2001), Chapter 7, Section 7.4, the (observed) dynamics of $\Lambda_t$ can then be expressed in terms of $\bar{B}_t$ as

$$d\Lambda_t/\Lambda_t = [\mu_L + P_t(\mu_H - \mu_L)]dt + \sigma d\bar{B}_t, \tag{2.4}$$

and by applying Itô's Lemma to (2.2), the dynamics of posterior beliefs can be obtained,

$$dP_t = P_t(1 - P_t)\frac{(\mu_H - \mu_L)}{\sigma}d\bar{B}_t. \tag{2.5}$$

A posterior belief satisfying (2.5) has a zero expected rate of change and at any point in time, the current belief is the best forecast of future belief. Indeed $\{P_t\}$ is an $(\mathbb{F}, P)$-(local)-martingale. Due to the fact that $P_t \in (0, 1)$, it is an $(\mathbb{F}, P)$-martingale. The variation in the posterior belief is proportional to the signal to noise ratio. When the noise ($\sigma$) is large, posterior beliefs change slowly since new observations convey little information about the growth rate $\mu$. When the difference between high and low growth rates, $\mu_H - \mu_L$, is large and the noise is small, new observations may reveal the true value of $\mu$ and the posterior belief experiences a large change.

*Remark I*: The Bayesian modelling framework considered here may be related to continuous-time Bayesian modeling frameworks used in, for example, Karatzas and Zhao (2001) and Zhang et al. (2012), to discuss optimization problems in mathematical finance and insurance.

*Remark II*: The compound Poisson process is widely used in the collective risk theory in actuarial mathematics to describe surplus processes of insurance companies, see, for example, the classic monograph by Bühlmann (1970). The compound Poisson process has also been used to value catastrophic insurance contracts.

[4]Note that the Brownian motion $\{B_t\}$ is not adapted to the filtration $\{\mathscr{F}_t, t \geq 0\}$, since $\mu$ is unknown and therefore, knowing the history of $\Lambda_t$ up to time $t$ is not sufficient to know the history of $B$ up to time $t$.

*2.2. Investments into Climate Change Adaptation*

Let us now consider an investment project with investment cost $I$ that is sunk once committed. The project reduces the frequency of catastrophic events by a proportion $k$ from the investment time until infinity. Since the expected loss over a period $(t_1, t_2]$, given the information observed up to and including time $t_1$, is $\beta E[\int_{t_1}^{t_2} \Lambda_s ds|\mathscr{F}_{t_1}]$, the investment payoff over this period is $k\beta E[\int_{t_1}^{t_2} \Lambda_s ds|\mathscr{F}_{t_1}]$. At the discount rate $r$, the expected NPV of investing in the project at time $\tau$ conditional on the information available up to and including time $t = 0$ is given by

$$E\left[k\beta \int_{\tau}^{\infty} e^{-rs}\Lambda_s ds - e^{-r\tau} I|\mathscr{F}_0\right]. \tag{2.6}$$

The decision maker determines an optimal time to enter into the investment project that maximizes the expected NPV. Admission investment times are non-anticipative (i.e., depend only on the current information, but not future information), which is the case if $\tau$ is a stopping time. Thus, if the current time is zero, the optimal investment problem can be formulated as:

$$\max_{\tau} E\left[k\beta \int_{\tau}^{\infty} e^{-rs}\Lambda_s ds - e^{-r\tau} I|\mathscr{F}_0\right] \tag{2.7}$$

subject to (2.4) and (2.5), and $\tau$ is an $\{\mathcal{F}_t\}$-stopping time taking a value in $[0, \infty)$.

In general, the performance functional may be formulated as:

$$\max_{\tau\in\Gamma_{t,\infty}} E\left[k\beta \int_{\tau}^{\infty} e^{-r(s-t)}\Lambda_s ds - e^{-r(\tau-t)} I|\mathscr{F}_t\right], \tag{2.8}$$

where $\mathscr{F}_t$ represents the information available up to and including time $t$ and $\Gamma_{t,\infty}$ is the space of all $\mathbb{F}$-stopping times taking a value in the interval $[t, \infty)$.

This problem has two state variables, $P_t$ and $\Lambda_t$ that are correlated. It may not be easy to directly calculate the NPV of a project invested at a given state. Determining the value of the option is even more difficult. In the following, we apply a change of measures method to simplify the problem.

*2.3. A Measure Change Approach*

The investment problem may now be simplified by changing the measure $P$ to $\tilde{P}$ under which $\Lambda_t$ has a known and constant growth rate of $\mu_H$. This measure change approach has been used in filtering and is called a reference probability approach, see, for example, Elliott et al. (1995). The measure change is achieved by using the Radon-Nikodym derivative $Z_\infty$ such that

$$\left.\frac{d\widetilde{P}}{dP}\right|_{\mathcal{F}_\infty} := Z_\infty, \tag{2.9}$$

where $Z_t = \exp\left(-\int_0^t \theta_s d\bar{B}_s - \frac{1}{2}\int_0^t \theta_s^2 ds\right)$, and $\theta_t = -(1-P_t)\omega$. Since $P_t \in (0,1)$, $|\theta_t|$ is bounded. Consequently, $\{Z_t\}$ is an $(\mathbb{F}, P)$-martingale. Indeed, it is an uniformly integrable martingale, and so $\lim_{t\to\infty} Z_t = Z_\infty$, $P$-a.s. Under $\tilde{P}$, $\tilde{B}_t = \bar{B}_t + \int_0^t \theta_s ds$ is a standard Brownian motion by Girsanov's theorem, (see, for example, Karatzas and Shreve (1988), Chapter 3, Section 3.5, and Elliott and Kopp (2005), Chapter 7, Section 7.2). To simplify the problem, we replace the state variable $P_t$ by the likelihood ratio $\phi_t = \frac{1-P_t}{P_t}$ that evolves over time according to the stochastic differential equation $d\phi_t = -\omega\phi_t d\tilde{B}_t$. By a version of the Bayes' rule, the investment problem then becomes

$$F(\phi_0, \Lambda_0) = \max_\tau \tilde{E}\left[\frac{1}{Z_\infty}\left(k\beta\int_\tau^\infty e^{-rs}\Lambda_s ds - e^{-r\tau}I\right)|(\phi_0,\Lambda_0)\right] \tag{2.10}$$

subject to the dynamic state constraints

$$d\Lambda_t/\Lambda_t = \mu_H dt + \sigma d\tilde{B}_t, \tag{2.11}$$

$$d\phi_t/\phi_t = -\omega d\tilde{B}_t. \tag{2.12}$$

Note that in (2.10), $\eta_t \equiv Z_t^{-1}$ has an initial starting point $\eta_0 = 1$ and evolves over time according to the stochastic differential equation $d\eta_t/\eta_t = \theta_t d\tilde{B}_t = d\phi_t/(1+\phi_t)$. Therefore, $\eta_t = \frac{1+\phi_t}{1+\phi_0}$ and $\phi_t$ is related to $\Lambda_t$ according to a time dependent relation (which is obtained by solving the differential equations (2.11) and (2.12)),

$$\frac{\phi_t}{\phi_0} = \left(\frac{\Lambda_t}{\Lambda_0}\right)^{-\omega/\sigma}\exp\left[\frac{\omega t}{2\sigma}(\mu_H + \mu_L - \sigma^2)\right]. \tag{2.13}$$

At the current state $(\phi_0, \Lambda_0)$, the actuarial value of the option to invest is

$$F(\phi_0, \Lambda_0) = \frac{1}{1+\phi_0} \max_{\tau} \tilde{E}\left[(1+\phi_\infty)\left(k\beta \int_\tau^\infty e^{-rs}\Lambda_s ds - e^{-r\tau} I\right) | (\phi_0, \Lambda_0)\right], \quad (2.14)$$

and when the state changes to $(\phi_t, \Lambda_t)$, by the Markov property, the actuarial value of the option becomes

$$F(\phi_t, \Lambda_t) = \frac{1}{1+\phi_t} \max_{\tau} \tilde{E}\left[(1+\phi_\infty)\left(k\beta \int_\tau^\infty e^{-r(s-t)}\Lambda_s ds - e^{-r(\tau-t)} I\right) | (\phi_t, \Lambda_t)\right]. \quad (2.15)$$

To find the value of the investment option, we solve the auxiliary optimal stopping problem:

$$G(\phi_t, \Lambda_t) = \max_{\tau \in \Gamma_{t,\infty}} \tilde{E}\left[(1+\phi_\infty)\left(k\beta \int_\tau^\infty e^{-r(s-t)}\Lambda_s ds - e^{-r(\tau-t)} I\right) | (\phi_t, \Lambda_t)\right], \quad (2.16)$$

where the intrinsic value obtained by stopping at time $t$, $V(\phi_t, \Lambda_t)$, is given by (see Appendix A for more details):

$$V(\phi_t, \Lambda_t) = k\beta\Lambda_t/(r-\mu_H) - (1+\phi_t)I + \phi_t k\beta\Lambda_t/(r-\mu_L). \quad (2.17)$$

Given state $(\phi_t, \Lambda_t)$, the decision to be made at time $t$ is whether to stop and get value $V(\phi_t, \Lambda_t)$ or to wait. Waiting to the next instant $t + \Delta t$ gives a value of

$$e^{-r\Delta t}\tilde{E}\left[G(\phi_{t+\Delta t}, \Lambda_{t+\Delta t}) | (\phi_t, \Lambda_t)\right].$$

The value $G(\phi_t, \Lambda_t)$ is the larger of the value obtained by immediate stopping and the value obtained by waiting,

$$G(\phi_t, \Lambda_t) = \max\{V(\phi_t, \Lambda_t), e^{-r\Delta t}\tilde{E}\left[G(\phi_{t+\Delta t}, \Lambda_{t+\Delta t}) | (\phi_t, \Lambda_t)\right]\}. \quad (2.18)$$

Suppose that the value function $G$ is "sufficiently" smooth in the continuation region, (i.e., deferring investment region). More specifically, $G \in \mathcal{C}^2$, where $\mathcal{C}^2$ is the space of twice continuously differentiable functions. Using Itô's lemma and standard arguments in optimal stopping theory, see, for example, Shiryaev (1978), Chapter 3, and Oksendal

(2003), Chapter 10, Section 10.4, (2.18) can be expressed as:

$$\max\Big(V(\phi_t,\Lambda_t)-G(\phi_t,\Lambda_t),\\ \frac{1}{2}\sigma^2\Lambda_t^2 G_{\Lambda\Lambda}+\frac{1}{2}\omega^2\phi_t^2 G_{\phi\phi}-\omega\sigma\phi_t\Lambda_t G_{\phi\Lambda}+\mu_H\Lambda_t G_\Lambda - rG\Big)=0, \tag{2.19}$$

where $G_\phi = \frac{\partial}{\partial\phi_t}G(\phi_t,\Lambda_t)$, $G_\Lambda = \frac{\partial}{\partial\Lambda_t}G(\phi_t,\Lambda_t)$, $G_{\phi\phi} = \frac{\partial^2}{\partial\phi_t^2}G(\phi_t,\Lambda_t)$, $G_{\Lambda\Lambda} = \frac{\partial^2}{\partial\Lambda_t^2}G(\phi_t,\Lambda_t)$ and $G_{\phi\Lambda} = \frac{\partial^2}{\partial\phi_t\partial\Lambda_t}G(\phi_t,\Lambda_t)$.

In the continuation region (i.e., deferring investment), the value of the option can be found by solving the second-order partial differential equation:

$$\frac{1}{2}\sigma^2\Lambda_t^2 G_{\Lambda\Lambda}+\frac{1}{2}\omega^2\phi_t^2 G_{\phi\phi}-\omega\sigma\phi_t\Lambda_t G_{\phi\Lambda}+\mu_H\Lambda_t G_\Lambda - rG=0. \tag{2.20}$$

In addition, at the optimal investment threshold $(\phi^*,\Lambda^*)$, the following high-contact and smooth-pasting conditions need to be satisfied [5]:

$$G(\phi^*,\Lambda^*)=V(\phi^*,\Lambda^*) \tag{2.21}$$

$$G_\phi(\phi^*,\Lambda^*)=V_\phi(\phi^*,\Lambda^*) \tag{2.22}$$

$$G_\Lambda(\phi^*,\Lambda^*)=V_\Lambda(\phi^*,\Lambda^*). \tag{2.23}$$

In general cases, the partial differential equation (2.20) may not have a closed form solution. The option value can be found by applying finite difference methods to (2.20) or a lattice method to (2.18). Note that for a lattice method, starting from an initial state $(\phi_0,\Lambda_0)$, the value of $\phi_t$ can be determined based on $\Lambda_t$, and the lattice has one state variable. This is much simpler than solving (2.20) with two state variables. We therefore use a binomial lattice method to calculate the option value and the optimal investment threshold. A binomial lattice is constructed by first fixing a time horizon $T$ and then dividing the time horizon into $N$ small sub-intervals, each of which has a time length of $\Delta t = T/N$. At an arbitrary time step $t$ of the binomial lattice, given the value $\Lambda_t$ of the

[5] In the context of pricing finite-maturity American-style contingent claims, some theoretical justifications for the high-contact and smooth-pasting conditions are available in the literature, see, for example, Elliott and Kopp (2005), Chapter 8, for the case of a geometric Brownian motion, and a recent paper by Siu (2016) for the case of a self-exciting threshold diffusion process.

Poisson intensity, the value $\Lambda_{t+\Delta t}$ of the Poisson intensity at the next time step $t+\Delta t$ is either $\Lambda_t u$ with probability $p$ or $\Lambda_t d$ with probability $1-p$, where $u = 1/d$. It is easy to see that the conditional mean and variance of $\Lambda_{t+\Delta t}$ given $\Lambda_t$ are $p\Lambda_t u + (1-p)\Lambda_t d$, and $\Lambda_t^2[pu^2 + (1-p)d^2 - [pu + (1-p)d]^2]$, respectively. As shown by Cox et al. (1979), these conditional mean and variance are the same as those implied by the stochastic differential equation (2.11), which are $\Lambda_t e^{\mu_H \Delta t}$ and $\Lambda_t^2 \sigma^2 \Delta t$, when $p$, $u$, and $d$ are set as follows:

$$u = e^{\sigma\sqrt{\Delta t}}, \qquad d = e^{-\sigma\sqrt{\Delta t}}, \qquad p = \frac{e^{\mu_H \Delta t} - d}{u - d}. \tag{2.24}$$

For a given initial condition $(\phi_0, \Lambda_0)$, the value $G(\phi_0, \Lambda_0)$ is computed by backward induction using Equation (2.18) starting with the terminal condition $G(\phi_{T+1}, \Lambda_{T+1}) = 0$. The computational efficiency of the lattice method can be improved by applying the Richardson extrapolation as suggested by Boyle et al. (1989). The value of the option is calculated for 20, 40, 60, and 80 time steps per year and the obtained points are then fitted with a cubic polynomial. The value given by the polynomial curve at a high number of time steps then provide an accurate estimate of the option value. In empirical work, we use an investment time horizon of 100 years, since it seems that further increasing the investment time horizon may not have a material effect on the solution.

### *2.4. Special Case*

As shown in (2.13), when $\mu_H + \mu_L = \sigma^2$, the two state variables of the investment problem map one to one in a time homogeneous relation. The problem has effectively one state variable $\Lambda_t$ and the optimal stopping time is the first time when $\Lambda_t$ exceeds the optimal threshold $\Lambda^*$. It is clear from (2.2) that in this special case, $\ln \Lambda_t$ follows an arithmetic Brownian motion.

#### *2.4.1. The Investment Threshold*

The partial differential equation (2.20) reduces to:

$$\frac{1}{2}\sigma^2 \Lambda_t^2 G_{\Lambda\Lambda} + \mu_H \Lambda_t G_\Lambda - rG = 0. \tag{2.25}$$

The value obtained by waiting is, therefore, $G(\Lambda_t) = A\Lambda_t^{\alpha_H}$, where $A$ is a parameter to be determined and $\alpha_H = \frac{1}{2} - \mu_H/\sigma^2 + \sqrt{(\mu_H/\sigma^2 - \frac{1}{2})^2 + 2r/\sigma^2}$. As a result, the high

contact and smooth pasting conditions at the optimal investment threshold $\Lambda^*$ become:

$$A\Lambda^{*\alpha_H} = \frac{k\beta\Lambda^*}{(r-\mu_H)} - I[1+\phi_0\left(\frac{\Lambda^*}{\Lambda_0}\right)^{-\omega/\sigma}] + \phi_0\left(\frac{\Lambda^*}{\Lambda_0}\right)^{-\omega/\sigma}\frac{k\beta\Lambda^*}{(r-\mu_L)}. \tag{2.26}$$

$$\begin{aligned} A\alpha_H\Lambda^{*\alpha_H-1} = &\frac{k\beta}{(r-\mu_H)} + I\phi_0\frac{\omega}{\sigma}\frac{1}{\Lambda^*}\left(\frac{\Lambda^*}{\Lambda_0}\right)^{-\omega/\sigma} + \phi_0\left(\frac{\Lambda^*}{\Lambda_0}\right)^{-\omega/\sigma}\frac{k\beta}{(r-\mu_L)} \\ &- \phi_0\frac{\omega}{\sigma}\left(\frac{\Lambda^*}{\Lambda_0}\right)^{-\omega/\sigma}\frac{k\beta}{(r-\mu_L)} \end{aligned} \tag{2.27}$$

Conditions (2.26) and (2.27) can be used to solve for the optimal investment threshold $\Lambda^*$ as well as the coefficient $A$ in the value $G(\Lambda_t)$. The optimal investment rule is to invest in period $t, t \geq 0$, if $\Lambda_t$ exceeds the threshold $\Lambda^*$ satisfying the following nonlinear equation:

$$\frac{P^*(\alpha_H-1)\frac{k\beta\Lambda^*}{r-\mu_H} + (1-P^*)(\alpha_L-1)\frac{k\beta\Lambda^*}{r-\mu_L}}{P^*\alpha_H + (1-P^*)\alpha_L} = I, \tag{2.28}$$

where $\alpha_i = \frac{1}{2} - \mu_i/\sigma^2 + \sqrt{(\mu_i/\sigma^2 - \frac{1}{2})^2 + 2r/\sigma^2}$ is the solution of the quadratic equation

$$\frac{1}{2}\sigma^2\alpha_i(\alpha_i-1) + \mu_i\alpha_i - r = 0, \qquad i \in \{H, L\}, \tag{2.29}$$

and $P^* = 1/(1+\phi^*)$, $\phi^* = \phi_0\left(\frac{\Lambda^*}{\Lambda_0}\right)^{-\omega/\sigma}$.

At the investment threshold, the ratio of belief weighted average of $(\alpha-1)V$ to the belief weighted average of $\alpha$ is equal to the investment cost[6], i.e. $\frac{E^*[(\alpha-1)V]}{E^*(\alpha)} = I$, where $E^*$ is the expectation under distribution $(P^*, (1-P^*))$ of the growth rate $(\mu_H, \mu_L)$. The consequence of having a back-loaded project instead of a front-loaded one is that the value of the project now depends on belief and the uncertain growth rate (see Equation (2.17)). This has an important implication: the investment threshold is decreasing in belief, rather than increasing in belief as for front-loaded projects, see Appendix B for more details. This means that the more pessimistic the decision maker is about the growth rate of the payoff flow, the longer she delays investment. This is in contrast with the investment behavior for front-loaded projects as documented by Décamps et al.

[6]When the growth rate is known, the optimal investment threshold satisfies $\frac{(\alpha-1)V}{\alpha} = I$, see, e.g. Dixit and Pindyck (1994).

(2005) and Klein (2009). Nevertheless this seems to be intuitively appealing.

*2.4.2. Option Value*

The value of the option in period $t$ is given by

$$F(P_t, \Lambda_t) = P_t \left(\frac{\Lambda_t}{\Lambda^*}\right)^{\alpha_H} \left(\frac{k\beta\Lambda^*}{r-\mu_H} - I\right) + (1-P_t)\left(\frac{\Lambda_t}{\Lambda^*}\right)^{\alpha_L} \left(\frac{k\beta\Lambda^*}{r-\mu_L} - I\right). \qquad (2.30)$$

The option value is a belief-weighted average of the corresponding values obtained in certainty cases. When $p_0 = 0$ or $p_0 = 1$, (2.28) and (2.30) provides the investment threshold and the option value for the case when the growth rate is known with certainty to be $\mu_L$ or $\mu_H$, which are consistent with the standard real options model outlined in Chapter 6 of Dixit and Pindyck (1994).

*2.4.3. Impacts of Uncertainty*

In this model, uncertainty about the growth of the Poisson intensity $\Lambda_t$ is represented by the spread $\mu_H - \mu_L$. Similar to Klein (2009), we found that uncertainty can increase or decrease the option value and the investment threshold of backloaded projects. This is illustrated for the special case where $\mu_H + \mu_L = \sigma^2$. With $\mu_H + \mu_L$ being kept constant, an increase in the uncertainty means that the high growth rate $\mu_H$ is increased by the same amount as the decrease in the low growth rate $\mu_L$. An increase in uncertainty is, therefore, corresponding to a mean preserving spread of the growth rate.

As shown in Figure 2, the impact of uncertainty on the investment threshold is non-linear and non-monotonic. It depends on the initial condition and the level of uncertainty. On the one hand, an increase in uncertainty results in a larger divergence between the option value with the high growth rate and the option value with the low growth rate. The benefit of waiting for more information is therefore increased and the investment threshold is raised to a higher level. On the other hand, an increase in uncertainty leads to a higher signal to noise ratio that speeds up uncertainty resolution, and reduces the waiting time. The direction of change for the investment threshold is dictated by the effect that dominates.

Similarly, the impact of uncertainty on the option value can be positive or negative,

depending on the actual changes in the option values with high and low growth rates and the change in the signal to noise ratio. It is interesting to note that the option value decreases at a slow rate when uncertainty is low, while increases at a high rate when uncertainty is sufficiently high (Figure 2). This is because an increase in uncertainty raises the high growth rate and reduces the low growth rate by the same amount. This increases the option value at the high growth rate with no limit, while it decreases the option value at a low growth rate towards zero. When the option value at the low growth rate is close to zero, it cannot be reduced beyond zero, and further increases in uncertainty will be translated into increases in the option value at the high growth rate. The value of the investment option, therefore, increases sharply.

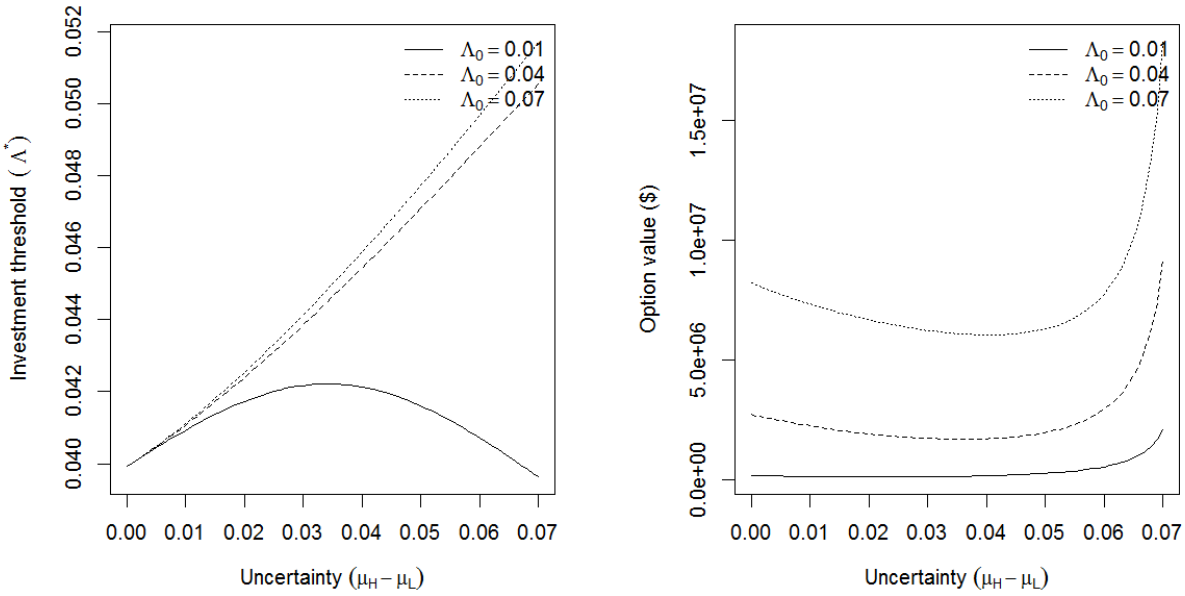


Figure 2: Impacts of uncertainty on the investment threshold and the option value for different initial values of Poisson intensity $\Lambda_0$.

*2.4.4. Learning Time*

When low and high growth rates have been determined, the expected time required to learn about the true growth rate with a level of confidence, e.g. 95% confidence, provides an indication of the speed of learning. We are $X\%$ confident that the true growth rate is $\mu_H$ when $P_t$ reaches $X\%$, or when $\Lambda_t$ reaches

$$\Lambda_H = \Lambda_0 \left( \frac{X(1-p_0)}{(100-X)p_0} \right)^{\sigma/\omega}.$$

The high threshold $\Lambda_H$ at which the high growth rate is revealed depends on the initial value of the Poisson intensity $\Lambda_0$ and the initial belief $p_0$. When the initial belief is equal to $X\%$, then $\Lambda_H$ is equal to $\Lambda_0$ and the true drift $\mu_H$ is learnt at the initial time. When $p_0 < X\%$, then $X(1-p_0)/(100-X)p_0 > 1$ and $\Lambda_H$ is equal to $\Lambda_0$ scaled up by a factor $(X(1-p_0)/(100-X)p_0)^{\sigma/\omega}$. The lower the signal to noise ratio, the higher the threshold $\Lambda_H$ relative to $\Lambda_0$, and the longer it takes to learn whether the true growth rate is $\mu_H$. The expected time for $\Lambda_t$ to reach $\Lambda_H$ from its current level $\Lambda_0$, when $\mu_H$ satisfies $\mu_H - \frac{1}{2}\sigma^2 > 0$ (see Appendix C), is:

$$E\tau_{\Lambda_H} = (\mu_H - \frac{1}{2}\sigma^2)^{-1} \ln \frac{\Lambda_H}{\Lambda_0}. \tag{2.31}$$

On the other hand, we are $X\%$ confident that the growth rate is $\mu_L$ when $1 - P_t$ reaches $X\%$, or $\Lambda_t$ reaches $\Lambda_L = \Lambda_0 \left(\frac{(100-X)(1-p_0)}{Xp_0}\right)^{\sigma/\omega}$. When $1 - p_0 = X\%$, then $\Lambda_L = \Lambda_0$ and the true growth rate is learnt at the initial time. In contrast, when $1 - p_0 < X\%$, then $(100-X)(1-p_0)/Xp_0 < 1$ and the threshold $\Lambda_L$ is $\Lambda_0$ scaled down by $\left(\frac{(100-X)(1-p_0)}{Xp_0}\right)^{\sigma/\omega}$. When the true growth rate is $\mu_L$ satisfying $\mu_L - \frac{1}{2}\sigma^2 < 0$, the expected time $E\tau_{\Lambda_L}$ for $\Lambda_t$ to reach $\Lambda_L$ can be obtained by using (2.31) with $\mu_L$ and $\Lambda_L$ replacing $\mu_H$ and $\Lambda_H$, respectively. When $\mu_L - \frac{1}{2}\sigma^2 \geq 0$, there is a positive probability that $\ln \Lambda_t$ wanders off to infinity and never goes down to $\ln \Lambda_L$. The expected time $E\tau_{\Lambda_L}$ is infinite and we expect not to know the true growth rate when it is $\mu_L$, although we may know it is not $\mu_L$ when $P_t$ reaches $X\%$.

Figure 3 provides an illustration of the expected time required to learn when $\mu_H = 0.015$, $\mu_L = 0$, $\sigma = 0.08$, $\Lambda_0 = 0.027$. When $p_0 = 0.5$ and $X = 95$, then $\Lambda_H = 0.095$ and $\Lambda_L = 0.008$. Although the current state $\Lambda_0$ is closer to $\Lambda_L$ than $\Lambda_H$, the expected time for $\Lambda_t$ to reach $\Lambda_L$ when $\mu = \mu_L$ (392 years) is much longer than the expected time for it to reach $\Lambda_H$ when $\mu = \mu_H$ (106 years). This is because the expected time is driven by the process $\{\ln \Lambda_t\}$, rather than $\{\Lambda_t\}$. Under the low growth rate, $\{\ln \Lambda_t\}$ has a much lower drift ($\mu_L - 0.5\sigma^2 = -0.0032$) and it takes a longer time to learn about the true rate than under the high growth rate ($\mu_H - 0.5\sigma^2 = 0.0118$).

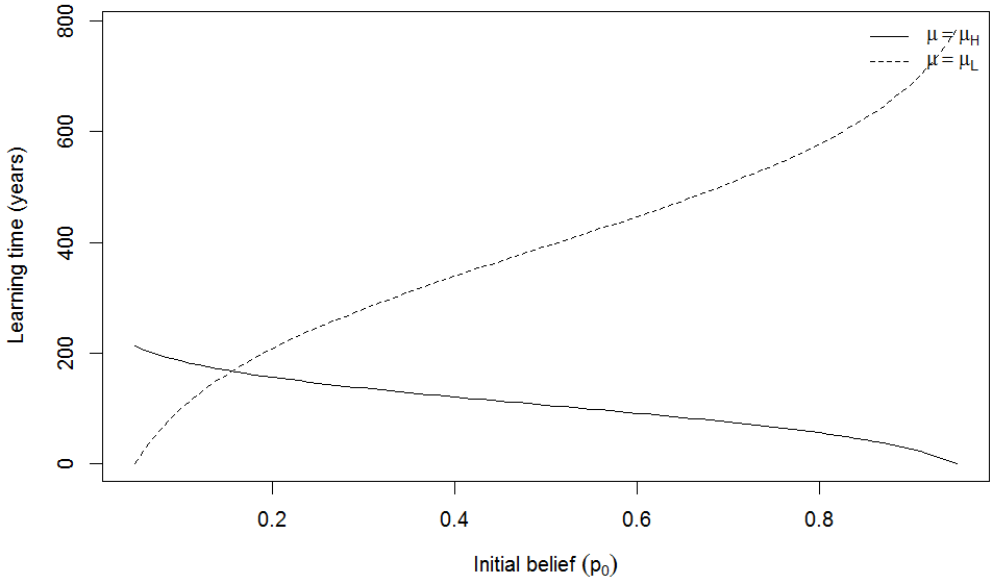


Figure 3: Expected time taken to learn about the true drift with 95% confidence when $\mu_H = 0.015$, $\mu_L = 0$, $\sigma = 0.08$ and $\Lambda_0 = 0.027$

*2.4.5. Expected Investment Delay*

The expected time to investment can be calculated as

$$E\tau_{\Lambda^*} = p_0 E[\tau_{\Lambda^*}|\mu = \mu_H] + (1 - p_0)E[\tau_{\Lambda^*}|\mu = \mu_L]. \tag{2.32}$$

Note that when $\mu_H - \frac{1}{2}\sigma^2 < 0$, $E[\tau_{\Lambda^*}|\mu = \mu_H]$ is infinite and as a result, the expected time to investment $E\tau_{\Lambda^*}$ is infinite. An important question is whether the real options framework is still relevant. This question can be answered by looking at the case $p_0 = 1$, i.e. the growth rate is known with certainty to be $\mu_H$, and the investment problem is reduced to the standard real options problem considered in the literature. If the volatility is positive, there may be a positive probability that the value of the project rises above the current level in the future and deferring investment to a later time may provide a higher value. As it is well-known from the real options literature, see, e.g. Dixit and Pindyck (1994), (and also apparent from (2.28)), when $\sigma > 0$, the investment threshold in terms of project value is $\frac{\alpha_H}{\alpha_H - 1} I$, which is higher than $I$. This holds regardless of the expected time to investment. The investment threshold given by our real options model is, therefore, optimal even when the expected investment delay or the expected time taken for uncertainty to resolve is infinite.

## 3. Empirical Application

In the following, we illustrate the application of the proposed model by examining a case study of bushfire risk management in Ku-ring-gai, a local area of Sydney, NSW, Australia. The area has residential properties in close proximity to bushland and ranks third in bushfire vulnerability among the 61 local government areas in the Greater Sydney Region.

A number of options has been identified by Ku-ring-gai Council to reduce the risk from bushfires. These include, among others, building new fire trails, constructing new fire stations and rezoning land, see Ku-ring-gai Council (2010). Fire trails allow for controlled hazard reduction burning, break wild fire transition and potentially allow more time for fire brigades to respond to bushfires. Constructing more fire stations reduces the response time and helps to reduce the risk of fires expanding beyond suppression. In the following, we will focus on evaluating an adaptation project of constructing an additional fire trail in the region.

### *3.1. Bushfire Risk Estimation*

Bushfires are rare events, especially at the local level, making the task of measuring fire risk particularly challenging. To establish a reliable relationship between observable climate variables and fire risk, we extend the statistical model to the national level, allowing us to use all bushfire events that have occurred in four states of Australia (ACT, NSW, VIC, TAS) since 1970. We use the database provided by Blanchi et al. (2010), where the location of events as well as additional information on the number of damaged houses and the associated weather conditions are reported. We combine these data with daily climate variables provided by the Bureau of Meteorology (Lucas, 2010) to form a daily data set for the estimation of bushfire frequency.

To relate the frequency of bushfires to the explanatory variables, we use a panel data Poisson generalized linear model:

$$P(Y_t^r = y^r) = \frac{(\Lambda_t^r)^{y^r} e^{-\Lambda_t^r}}{y^r!}, \quad r = \text{ACT, NSW, VIC, TAS,} \tag{3.1}$$

where $Y_t^r$ is the number of bushfire events occurring in region $r$ in period $t$ and $\Lambda_t^r$ is the intensity parameter that controls the probability of a catastrophic event in region $r$ in period $t$.

In the following, we assume that the square root[7] of the parameter $\Lambda_t^r$ of the Poisson distribution depends linearly on $q$ covariates for region $r$:

$$\begin{bmatrix} \sqrt{\Lambda_t^{ACT}} \\ ... \\ \sqrt{\Lambda_t^{TAS}} \end{bmatrix} = \begin{bmatrix} 1 & X_{1,t}^{ACT} & X_{2,t}^{ACT} & ... & X_{q,t}^{ACT} \\ ... & ... & ... & ... & ... \\ 1 & X_{1,t}^{TAS} & X_{2,t}^{TAS} & ... & X_{q,t}^{TAS} \end{bmatrix} \begin{bmatrix} \gamma_0 \\ \gamma^{X_1} \\ \gamma^{X_2} \\ ... \\ \gamma^{X_q}. \end{bmatrix}. \tag{3.2}$$

To account for the persistent impact that weather has on bushfire risk, we construct weighted variables for rainfall, maximum temperature and for the number of fires that occurred in the last $m$ days, where $m = 7, 15, 22, 30$. To allocate more weight to more recent observations of the variables, we use a weighting scheme, where the weight decreases linearly from $m/\sum_{i=1}^{m} i$ for the current day to $1/\sum_{i=1}^{m} i$ for the day that is $m-1$ days before the current day. The weighted rainfall and weighted maximum temperature utilize observations of the current day, while the weighted number of fires is constructed from the lags of the number of fires and does not include the number of fires observed on the current day. In addition, we include national GDP as a proxy for risk mitigation activities, state dummies to reflect the impact of region-specific factors that are not included in the model and a fire season dummy to represent the different impacts of seasons.

We select the included variables based on the generalized Akaike information criterion (GAIC) introduced by Rigby and Stasinopoulos (2005). The GAIC is defined as $-2 \times loglik + kp$, where $p$ is the total number of effective degrees of freedom used in the model and $k$ represents the penalty applied to each degree of freedom. When $k = 2$,

[7]Note that alternatively to a square root link function, a log link or an identity link function could have been used. However, for the log link function, the Poisson intensity is an exponential function of covariates and small variations in the covariates may cause excessive variation in the Poisson intensity. For the identity link, the Poisson intensity may be negative for non-average values of covariates.

GAIC reduces to the standard AIC, and when $k$ is increased to $\ln n$, where $n$ is the number of observations, GAIC becomes the Bayesian information criterion (BIC). Using the AIC often results in including also insignificant covariates, while using the BIC may exclude significant explanatory variables. To obtain an appropriate set of covariates for a given model, we increase the level of penalty $k$ from 2 until all insignificant covariates are excluded or until $\ln n$ is reached.

Table 1 provides the estimation results for the Poisson regression model. It is found that maximum temperature and wind speed on the current day are significant at the 5% level and the weighted number of bushfires in the last 30 days is significant at the 10% level. The model has a reasonable pseudo $R^2$ of 27%[8].

Table 1: Poisson Regression Results

| Explanatory Variable | Parameter | |
|---|---|---|
| Intercept | -0.0701 | *** |
| $\text{tmax}_t^r$ | 0.0028 | *** |
| $\text{wind}_t^r$ | 0.001 | *** |
| $\text{Y30}_t^r$ | 0.0021 | ** |
| Pseudo $R^2$ | 0.2734 | |

Note: Significance at the 1%, 5% and 10% level is denoted by ***, ** and *, respectively.

The risk of bushfire occurrence in the study region is estimated by downscaling the risk that has been estimated for NSW. In the Ku-ring-gai area, there was only one bushfire event over the last 40 years, and the Poisson intensity for the fire risk in Ku-ring-gai is obtained by scaling down the NSW fire risk by a factor of 10 so that the total risk in Ku-ring-gai over 40 years is equal to 1. Note that the annual risk for the local area is obtained by aggregating daily risks. The estimated volatility of the annual risk is 43% and the current value of the Poisson intensity for the region is 0.027.

The growth rate of the Poisson intensity is estimated based on a climate change skeptic view that suggests $\mu_L = 0$, i.e. no climate change, and a climate change study that

[8]We use McFadden's $R^2 = 1 - \ell_1/\ell_0$, where $\ell_1$ is the loglikelihood of the model with the included covariates and $\ell_0$ is the loglikelihood of the model without any covariates (McFadden, 1973).

suggest a value $\mu_H > 0$. We adopt the results of Hasson et al. (2009) who uses 10 general circulation models together with a low (B1) and a high (A2) GHG emission scenario to study the changes in the frequency of extreme fire weather events in southeastern Australia. The value of $\mu_H$ is set to equal to the average growth rate of 1.59% found by Hasson et al. (2009).

To estimate the number of houses damaged in a fire event in the area, we use quantile regression proposed by Koenker and Bassett (1978) to relate the number of damaged houses to risk exposure (the number of houses in a region) and other factors. The regression model for a quantile level $\tau \in (0, 1)$ can be formally written as

$$Q^{\tau}(Y|X) = \delta_0^{(\tau)} + \delta_1^{(\tau)} X_1 + ... + \delta_K^{(\tau)} X_K, \tag{3.3}$$

where $Q^{\tau}(Y|X)$ is the $\tau$-quantile of the conditional (on covariates' levels) distribution of the response variable $Y$. The response variable is the natural logarithm of the number of damaged houses. Quantile regression is more flexible than the usual OLS regression since it does not assume a distributional form for the response variable and covariates are allowed to affect not only the mean, but also higher order moments of the distribution. This framework is especially suitable for the current context of catastrophic risks, since losses are often found to be heavy tailed, rather than following a normal distribution (Lave and Apt, 2006).

Regression results are shown in Table 2. We found that the total number of houses and GDP have significant impacts on low quantile losses, while maximum temperature, GDP and wind speed have significant impacts on high quantile losses. The pseudo $R^2$s for different levels of $\tau$ suggest that the estimated quantile regression models have a reasonably high explanatory power.[9]

[9]Note that in conducting regression for multiple levels of quantiles, we obtain a discrete distribution of loss severity. Pseudo $R^2$ is calculated based on the goodness of fit of the model with and without

Table 2: Quantile regression results for lost houses

| | Explanatory Variable | | | | | | | | |
|---|---|---|---|---|---|---|---|---|---|
| Quantile level | Intercept | lnhouse | | gdp | | $\text{tmax15}_t^r$ | | $\text{wind}_t^r$ | | Pseudo $R^2$ |
| $\tau = 0.1$ | -5.46 | 0.55 | | -6.72 | | 0.09 | | -0.06 | | 0.16 |
| $\tau = 0.2$ | -5.54 | 0.6 | * | -6.56 | | 0.05 | | -0.03 | | 0.19 |
| $\tau = 0.3$ | -7.98 | 0.74 | ** | -8.28 | ** | 0.05 | | 0.01 | | 0.19 |
| $\tau = 0.4$ | -7.95 | 0.55 | | -10.6 | ** | 0.16 | | 0.01 | | 0.18 |
| $\tau = 0.5$ | -3.02 | 0.2 | | -10.79 | ** | 0.16 | | 0.01 | | 0.18 |
| $\tau = 0.6$ | -4.24 | 0.21 | | -9.75 | ** | 0.18 | | 0.02 | | 0.19 |
| $\tau = 0.7$ | -7.36 | -0.21 | | -8.31 | | 0.4 | * | 0.09 | ** | 0.21 |
| $\tau = 0.8$ | -4.11 | -0.34 | | -10.69 | * | 0.41 | ** | 0.07 | * | 0.29 |
| $\tau = 0.9$ | -4.48 | -0.33 | | -6.59 | | 0.46 | *** | 0.02 | | 0.41 |

Note: Significance at the 1%, 5% and 10% level is denoted by ***, ** and *, respectively.

The expected number of damaged houses for Ku-ring-gai in a fire event is estimated as 59 houses. This number of damaged houses and the re-construction cost of $422,000 per house are used to calculate the expected loss $\beta$ [10].

### *3.2. The Discount Rate*

The choice of an appropriate discount rate for long lasting projects is a highly controversial topic in the literature. Some studies, e.g. Stern (2007) and Garnaut (2008), recommend the use of low social discount rates, largely based on intergenerational equity arguments, while others such as Newell and Pizer (2003), Nordhaus (2007), Quiggin (2008) and Tol and Yohe (2009) suggest that the discount rate should be derived based

covariates:

$$R = 1 - \frac{V_1^{(\tau)}}{V_0^{(\tau)}},$$

$$V_1^{(\tau)} = \sum_{Y_i \geq X_i\hat{\delta}^{(\tau)}} \tau|Y_i - X_i\hat{\delta}^{(\tau)}| + \sum_{Y_i < X_i\hat{\delta}^{(\tau)}} (1-\tau)|Y_i - X_i\hat{\delta}^{(\tau)}|$$

$$V_0^{(\tau)} = \sum_{Y_i \geq \hat{Q}^{(\tau)}(Y)} \tau|Y_i - \hat{Q}^{(\tau)}(Y)| + \sum_{Y_i < \hat{Q}^{(\tau)}} (Y)(1-\tau)|Y_i - \hat{Q}^{(\tau)}(Y)|$$

[10]Note that the actual cost of damage can be more than the reconstruction cost when house contents are taken into account. However, without detailed insurance claim data, we cannot estimate the cost of house contents as well as its growth rate. Increases in daily maximum temperature is predicted to increase the number of damaged houses but the expected loss can still be increasing or decreasing since GDP growth reduces the number of damaged houses while at the same time it will most likely increase the value of damaged house contents. In this paper, we focus on the stochastic component of bushfire frequency and assume that the expected loss is constant.

on market interest rates.

Similar to Truong and Trück (2016), we adopt the approach proposed by Newell and Pizer (2003) to determine the appropriate discount rate for investment valuation. This approach estimates the discount rate using data on the prices of long term government bonds. Since the prices of government bonds vary stochastically over time, risk free interest rates are also stochastic. Newell and Pizer (2003) and Groom et al. (2007) show that when interest rates are stochastic and persistent, the certainty equivalent discount rate is decreasing over time, which is consistent with hyperbolic discounting behaviour observed by Frederick et al. (2002).

Truong and Trück (2016) estimate the stochastic interest rate model proposed by Cox et al. (1985) using long term Australian government bond data. They found that for Australian interest rates the estimated model yields a quite low persistent coefficient, and the estimated certainty equivalent discount rate converges quickly to a long run level of 4.5%. For simplicity, in this study, we assume that the discount rate is constant at 4.5%.

### *3.3. Other Parameters*

Other parameters relating to the investment project, including investment cost, risk mitigation effectiveness and project life, are estimated by expert elicitation. Expert elicitation is an effective way to overcome data scarcity problems and has been used in many previous climate adaptation studies, see e.g. Baker and Solak (2011); Mathew et al. (2012). The expert specifies that the conducted project is expected to reduce the frequency of house damaging bushfire events by 20%. The estimated costs for a finite lifetime project in Table 3 can be used to calculate the investment cost of an infinite lifetime project by firstly converting the investment cost $I_M$ of a project that lasts $M$ years into an annuity flow, $A$:

$$A = I_M \frac{1-\beta}{1-\beta^{M+1}}, \qquad \beta = 1/(1+r),$$

Table 3: Information on estimated and assumed parameter values, including the initial value of the Poisson intensity $\Lambda_0$, values for the high Poisson intensity growth rate $\mu_H$, the low Poisson intensity growth rate $\mu_H$, the volatility of the Poisson intensity process $\sigma$, the expected loss conditional on a bushfire event $\beta$, the risk mitigation of the project with respect to the frequency of house damaging bushfire events $k$, the assumed lifetime of the investment project $M$, the investment cost per project $I_M$, the annual maintenance cost for the project $C$, and the applied discount rate $r$.

| Parameters | Value |
|---|---|
| Current Poisson intensity ($\Lambda_0$) | 0.027 |
| High Poisson intensity growth ($\mu_H$) | 1.59% |
| Low Poisson intensity growth ($\mu_L$) | 0% |
| Volatility ($\sigma$) | 43% |
| Expected loss conditional on a fire event ($\beta$) | \$24,898,000 |
| Risk mitigation by project ($k$) | 20% |
| Lifetime of the project ($M$) | 50 years |
| Investment cost per project ($I_M$) | \$1.5 million |
| Project maintenance cost ($C$) | \$50,000 |
| Discount rate ($r$) | 4.5% |

and use the annuity $A$ is to calculate the investment cost of an infinite life project:

$$I = A(1 + r)/r. \tag{3.4}$$

Thus, at a 4.5% discount rate, the present value of building a bushfire trail every 50 years, each costing \$1.5 million to build is \$1.68 million.

### *3.4. Empirical Results*

#### *3.4.1. Baseline Case*

Figure 4 provides the plot of the option value $F(\Lambda_0)$ for the baseline set of parameters where the initial belief is $P_0 = 0.5$. For this case, at the current level of Poisson intensity $\Lambda_0 = 0.027$, the option value is \$1,472,731 and the optimal investment threshold for the initial period is $\Lambda^* = 0.0914$. Given the large volatility, the expected time to learn about the growth rate with 95% confidence when it is $\mu_L$ is 370 years, while the expected time to learn when the true growth rate is $\mu_H$ and the expected time to investment are both infinitely large. Recall, however, that the infinite expected time to learn and to invest do not affect the validity of the real options model as discussed above.

The investment threshold obtained from the model is substantially higher than the thresh-

old given by the NPV rule ($\Lambda_0 = 0.02$). If the NPV rule was used, the project would be invested immediately, and a NPV of \$1,015,149 would be obtained. An amount of \$457,582, i.e. 31.07% of the option value would be lost. For other levels of belief, optimal investment decisions can be made based on the investment boundary in Figure 5. For example, if $\Lambda_0 = 0.089$ and $P_0 = 0.4$, the optimal decision is to wait, while if $\Lambda_0 = 0.094$ and $P_0 = 0.8$, the project should be invested. When $\Lambda_0$ is lower than 0.089 (higher than 0.095), waiting (investing) is optimal regardless of belief.

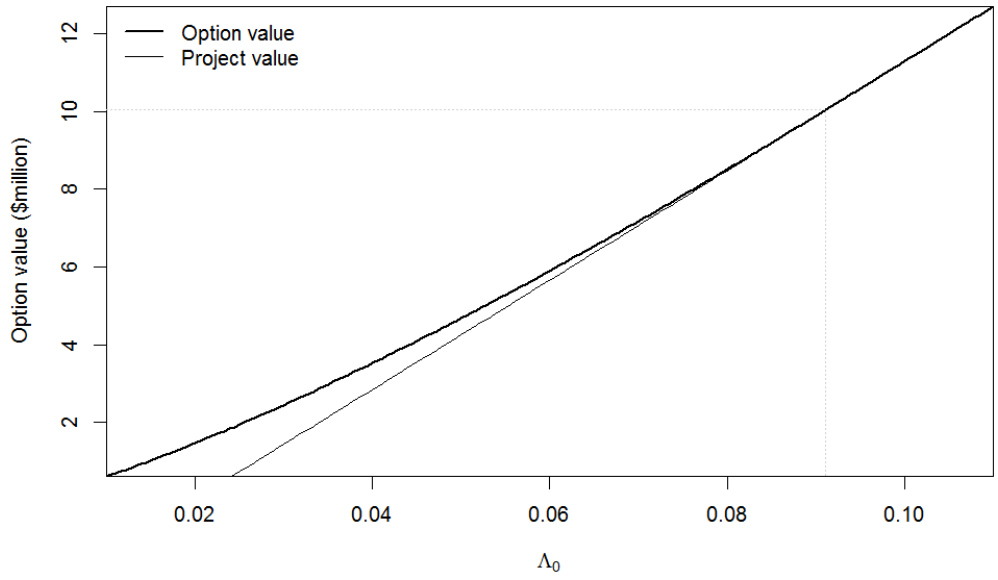


Figure 4: Investment option values, project values and investment threshold in baseline case with $P_0 = 0.5$

*3.4.2. Impact of Initial Belief*

To enable a comparison with the impact of other factors, we examine the impact of an increase in the initial belief $P_0$ by 10% from 0.5. For this higher belief, the investment threshold is slightly lower at $\Lambda^* = 0.0906$ and the option value at $\Lambda_0 = 0.027$ is increased by 0.5% to \$1,480,152. The NPV of the project at $\Lambda_0 = 0.027$ is increased by 8.04% to \$1,096,773 and the loss due to using the NPV rule is reduced by 16.22% to \$383,379.

*3.4.3. Impact of Uncertainty*

The impact of uncertainty is examined by comparing the baseline scenario with the case where uncertainty is increased by 10%, i.e. $\mu_L$ is decreased to -0.0795% and $\mu_H$ is

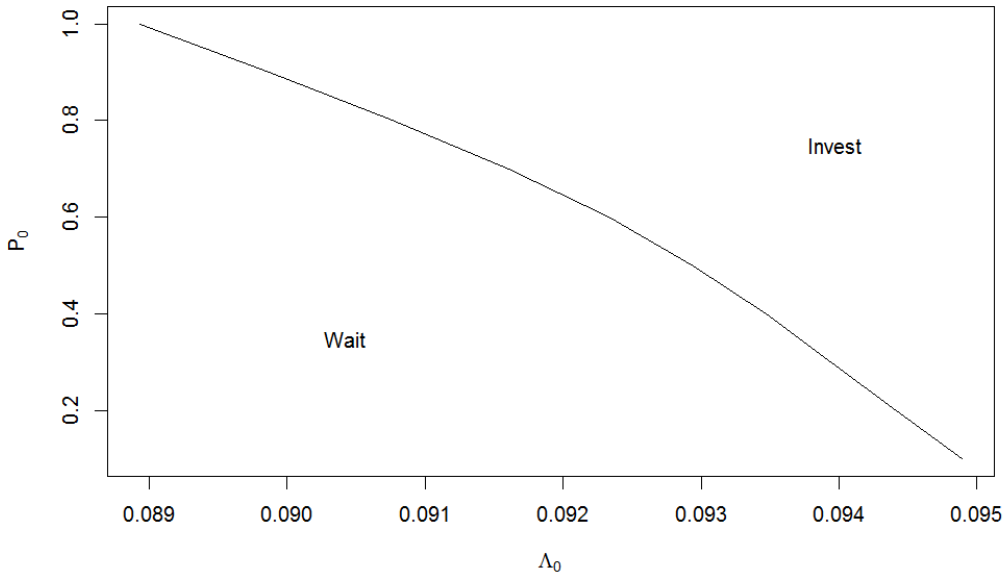


Figure 5: Investment boundary defined in two states $(P_0, \Lambda_0)$

increased to 1.6695%. When the uncertainty increases by 10%, the NPV of the project at the initial state $(P_0 = 0.5, \Lambda_0 = 0.027)$ increases by 3.84%. This is because the NPV of the project is $V(\phi_0, \Lambda_0)/(1 + \phi_0)$, and as can be seen from (2.17), $V(\phi_0, \Lambda_0)$ is a convex function of a random variable $\mu$ that takes values $\{\mu_H, \mu_L\}$. Therefore, when the uncertainty in $\mu$ increases, the NPV of the project increases. In contrast, the option value at the initial state decreases by 2.47% to \$1,436,386 and the optimal investment threshold decreases slightly to 0.0911. The loss due to using the NPV rule is reduced by 16.46% to \$382,287.

*3.4.4. Impact of Volatility*

When $\mu$ is known and constant, it is well known from the real options literature that the value of the option increases with the volatility $\sigma$. For the case of incomplete information where the true value of $\mu$ is unknown, volatility affects the value of the option through two different channels, that will either lead to an overall positive or negative impact on the option value. On the one hand, a higher volatility will increase the value of the option in certainty cases i.e. $\mu = \mu_H$ or $\mu = \mu_L$. On the other hand, a higher volatility will reduce the signal to noise ratio $\omega$ and reduce the value of the option. The net impact will depend on the empirical set of parameters. For the current application, when volatility increases by 10%, under the assumption of risk neutrality, the NPV of the project at the initial state

$(P_0 = 0.5, \Lambda_0 = 0.027)$ remains unchanged. The optimal investment threshold increases significantly to 0.1017 while the option value at the initial state increases by 6.63% to \$1,570,317. As a result, the loss incurred when using the NPV rule in comparison to optimal timing of the investment increases by 21.33% to \$555,169.

*3.4.5. Impact of Climate Change Scenarios*

Some climate change studies, e.g. Weitzman (2009); Keller et al. (2004), suggest that the extent of change in the future climate may be larger than predicted by statistical models. We examine a more serious climate change scenario in which the high level of the growth rate, $\mu_H$, is increased by 10%. With the increase in $\mu_H$, the NPV of the project at the initial state $(P_0 = 0.5, \Lambda_0 = 0.027)$ increases by 13.15% to \$1,148,667. The option value at the initial state is increased by 0.85% to \$1,485,319 and the investment threshold is reduced slightly to 0.0905. Under these assumptions, the loss incurred by using the NPV rule is then reduced by 26.43% to \$336,652.

*3.4.6. Impact of Investment Costs*

When the investment cost increases by 10%, the NPV of the project at the initial state $(P_0 = 0.5, \Lambda_0 = 0.027)$ is decreased by 27.47% to \$736,263. The option value at the initial state is reduced by 3.24% and the investment threshold increases to 0.1006. The loss due to using the NPV rule in comparison to the optimal timing of the investment is then increased by 50.53% to \$688,788. Therefore, changes in the initial investment cost may have a substantial impact on the value obtained from investing and the time when the project should be invested.

*3.4.7. Impact of the Discount Rate*

The impact of the applied discount rate on the results is examined by comparing the baseline scenario with the case where the discount rate is increased by 10%. As a result of the higher discount rate, the NPV of the project at the initial state $(P_0 = 0.5, \Lambda_0 = 0.027)$ is decreased by 30.14% to \$709,192. The investment threshold is decreased to 0.09 and the option value at the initial state is significantly reduced by 14.10% to \$1,265,087. The loss due to using the NPV rule therefore increases by 21.49% to \$555,894.

Table 4: Sensitivity Analysis for a 10% increase in key parameters: the parameter for initial belief $P_0$ is changed from $P_0 = 0.50$ to $P_0^* = 0.55$; to measure the sensitivity of the results to uncertainty, $\mu_H - \mu_L$ changes from 0.0159 to 0.0175 corresponding to $\mu_L^* = -0.0795\%$ and $\mu_H^* = 1.6695\%$; to examine the impact of volatility, $\sigma$ is increased from $\sigma = 0.43$ to $\sigma^* = 0.473$; to quantify the impact of a more serious climate change scenario, $\mu_H$ increases from 1.59% to 1.75%; investment costs are assumed to increase from $I_m = \$1,500,000$ to $I_m^* = \$1,650,000$; the discount rate $r$ changes from $r = 0.045$ to $r^* = 0.0495$.

| Parameter | ΔNPV | Δ(Option value) | Δ(Investment threshold) | Δ(Loss by NPV rule) |
|---|---|---|---|---|
| Initial belief ($P_0$) | 8.04% | 0.50% | -0.87% | -16.22% |
| Uncertainty ($\mu_H - \mu_L$) | 3.84% | -2.47% | -0.33% | -16.46% |
| Volatility ($\sigma$) | 0.00% | 6.63% | 11.27% | 21.33% |
| Climate Change ($\mu_H$) | 13.15% | 0.85% | -0.98% | -26.43% |
| Investment cost ($I_m$) | -27.47% | -3.24% | 10.07% | 50.53% |
| Discount rate ($r$) | -30.14% | -14.10% | -1.53% | 21.49% |

*3.4.8. Summary of sensitivity analysis*

A summary of the results for the conducted sensitivity analysis is provided in Table 4. Recall that for each variable we examine the impact of a 10% increase in the parameter value. For our case study we find that the loss due to using a simple NPV rule instead of optimally timing the investment increases substantially for a higher value of volatility, a larger initial investment cost, and an increased discount rate. In addition, the loss is decreasing in the signal to noise ratio, i.e. the loss is higher when the uncertainty is low or when the volatility is high. This means that the real options model is more important in settings where uncertainty resolution is slow. Furthermore, the loss is decreasing in the initial belief in climate change as well as the predicted level of climate change, which is consistent with the findings of Truong and Trück (2016).

## 4. Conclusion

In this paper, we introduce a novel framework for determining the optimal investment timing of catastrophic risk mitigation projects. The model can incorporate the impact of uncertainty in the growth rate of the expected frequency of catastrophic events and continuous Bayesian information updating into investment decisions. In addition, we provide closed form solutions for the investment problem when the logarithm of invest-

ment payoff follows a random walk process without drift. The investment threshold is determined in line with a standard real options model with the uncertain components evaluated at their belief weighted averages. In this model, uncertainty can accelerate or decelerate investment and can increase or decrease the option value, depending on the estimated values of the model parameters. We show that even when the expected time for the uncertainty to resolve is infinitely long, it is still relevant to use the proposed model instead of a standard net present value rule for investment decisions.

We illustrate the application of the model, using a case study of bushfire risk management in a local government area in Sydney, Australia. Catastrophic risk is quantified using a Poisson panel data model for loss frequency and quantile regression for the loss severity. We find that ignoring the option to defer the investment would result in a significant loss in comparison to an optimally timed investment. Sensitivity analysis results suggest that the loss is large when the investment cost is high, when the uncertainty resolves slowly over time, when the belief in climate change, or when the predicted extent of climate change is low. The real options model is therefore most useful for large investment projects whose benefits depend on future climate and the decision maker has a low belief about the climate change scenario.

The high sensitivity of the option value and the loss incurred by using the NPV rule to volatility changes may also provide practical ground for the development of real options models with volatility uncertainty. This may represent interesting topics for future research.

## Appendix A. Immediate Stopping Value

The immediate stopping value $V(\phi_t, \Lambda_t)$ is obtained by setting the stopping time $\tau$ to $t$ in (2.16),

$$\begin{aligned} V(\phi_t, \Lambda_t) &= \tilde{E}\left[(1+\phi_\infty)\left(k\beta\int_t^\infty e^{-r(s-t)}\Lambda_s ds - I\right)|(\phi_t, \Lambda_t)\right] \\ &= \tilde{E}\left(k\beta\Lambda_t/(r-\mu_H) - (1+\phi_\infty)I + \phi_\infty k\beta\int_t^\infty e^{-r(s-t)}\Lambda_s ds|(\phi_t, \Lambda_t)\right). \quad \text{(A.1)} \end{aligned}$$

Since $\phi_\infty$ can be expressed as a product of $\phi_t$ and a martingale (which follows from (2.13)),

$$\phi_\infty = \lim_{T\to\infty}\phi_T = \lim_{T\to\infty}\phi_t \exp\left(-\frac{1}{2}\omega^2(T-t) - \omega(\widetilde{B}_T - \widetilde{B}_t)\right), \quad \text{(A.2)}$$

and the last component in (A.1) can be written as

$$\phi_t\hat{E}\left(k\beta\int_t^\infty e^{-r(s-t)}\Lambda_s ds|(\phi_t, \Lambda_t)\right), \quad \text{(A.3)}$$

where $\hat{E}$ is the expectation under measure $\hat{P}$ given by

$$\left.\frac{d\hat{P}}{d\widetilde{P}}\right|_{\mathcal{F}_\infty} := \hat{Z}_\infty,$$

and $\hat{Z}_\infty = \lim_{T\to\infty}\exp\left(-\frac{1}{2}\omega^2(T-t) - \omega(\widetilde{B}_T - \widetilde{B}_t)\right)$. Under measure $\hat{P}$, the process $\{\Lambda_s\}$ has a constant growth rate $\mu_L$. The value obtained by immediate stopping becomes

$$V(\phi_t, \Lambda_t) = k\beta\Lambda_t/(r-\mu_H) - (1+\phi_t)I + \phi_t k\beta\Lambda_t/(r-\mu_L). \quad \text{(A.4)}$$

## Appendix B. Investment boundary

We show that in the special case ($\mu_H+\mu_L = \sigma^2$), the investment threshold $\Lambda^*$ is decreasing in belief $P^*$. Using (2.28) to find the derivative of $\Lambda^*$ with respect to $P^*$, it can be verified that $d\Lambda^*/dP^*$ has the same sign as

$$D = \frac{\alpha_L - 1}{r - \mu_L}\alpha_H - \frac{\alpha_H - 1}{r - \mu_H}\alpha_L. \tag{B.1}$$

Since $\alpha_i$ satisfies (2.29), it follows that $\frac{\alpha_i - 1}{r-\mu_i} = \frac{\alpha_i}{\frac{1}{2}\sigma^2\alpha_i + r} \quad i \in \{H, L\}$, and we have

$$D = \frac{\frac{1}{2}\sigma^2\alpha_H\alpha_L(\alpha_H - \alpha_L)}{(\frac{1}{2}\sigma^2\alpha_H + r)(\frac{1}{2}\sigma^2\alpha_L + r)}. \tag{B.2}$$

Since $\mu_H + \mu_L = \sigma^2$, it can be shown that $\alpha_L = \alpha_H + \omega/\sigma$ and therefore $\alpha_L > \alpha_H > 0$. As a result, $D < 0$ and $d\Lambda^*/dP^* < 0$.

## Appendix C. Expected waiting time

For a process $dX_t = adt + \sigma dB_t$, where $B_t$ is a Brownian motion, $X_0 = x > 0$, a stopping time $\tau_m = \min\{t \geq 0 : X_t = m\}$, and a scalar $u > 0$,

$$Ee^{-u\tau_m} = \exp\left[\frac{-a + \sqrt{a^2 + 2u\sigma^2}}{\sigma^2}(x - m)\right]. \tag{C.1}$$

Then, taking the limit $\lim_{u\downarrow 0} \frac{\partial Ee^{-u\tau_m}}{\partial u}$ gives

$$E\tau_m = \frac{m - x}{a}. \tag{C.2}$$

This result holds if $a > 0$ when $x < m$ or if $a \leq 0$ when $x > m$. The reason is if $a \leq 0$ when $x < m$, there is a positive probability that the process $X_t$ wanders off to $-\infty$ and $E\tau_m$ is infinite.

Applying the above result to the process $\lambda_t = \ln \Lambda_t$ that has drift $a = \mu_H - \frac{1}{2}\sigma^2$ and the hitting boundary $m = \ln \Lambda_H$, the expected waiting time becomes

$$E\tau_{\Lambda_H} = (\mu_H - \frac{1}{2}\sigma^2)^{-1} \ln \frac{\Lambda_H}{\Lambda_0}. \tag{C.3}$$

For the proof of (C.1), see e.g. Ryan and Lippman (2003).

*References*


Baker, E., Solak, S., 2011. Climate change and optimal energy technology R&D policy. European Journal of Operational Research 213 (2), 442–454.

Blanchi, R., Lucas, C., Leonard, J., Finkele, K., 2010. Meteorological conditions and wildfire-related house loss in Australia. International Journal of Wildland Fire 19 (7), 914–926.

Bouwer, L. M., Bubeck, P., Aerts, J. C., 2010. Changes in future flood risk due to climate and development in a Dutch polder area. Global Environmental Change 20 (3), 463–471.

Boyle, P. P., Evnine, J., Gibbs, S., 1989. Numerical evaluation of multivariate contingent claims. Review of Financial Studies 2 (2), 241–250.

Brouwer, R., van Ek, R., 2004. Integrated ecological, economic and social impact assessment of alternative flood control policies in the Netherlands. Ecological Economics 50 (1-2), 1–21.

Bühlmann, H., 1970. Mathematical methods in risk theory. Springer, New York.

Carey, J. M., Zilberman, D., 2002. A model of investment under uncertainty: modern irrigation technology and emerging markets in water. American Journal of Agricultural Economics 84 (1), 171–183.

Chao, P. T., Hobbs, B. F., 1997. Decision analysis of shoreline protection under climate change uncertainty. Water Resources Research 33 (4), 817–829.

Collins, D., Della-Marta, P., Plummer, N., Trewin, B., 2000. Trends in annual frequencies of extreme temperature events in Australia. Australian Meteorological Magazine 49 (4), 277–292.

Cox, J. C., Ingersoll, J. E., Ross, S. A., 1985. A theory of the term structure of interest rates. Econometrica 53 (2), 385–407.

Cox, J. C., Ross, S. A., Rubinstein, M., 1979. Option pricing: A simplified approach. Journal of Financial Economics 7 (3), 229–263.

Décamps, J.-P., Mariotti, T., Villeneuve, S., 2005. Investment timing under incomplete information. Mathematics of Operations Research 30 (2), 472–500.

Dixit, A. K., Pindyck, R. S., 1994. Investment under uncertainty. Princeton University Press, Princeton, New Jersey.

Elliott, R., Kopp, K., 2005. Mathematics of Financial Markets, 2nd Edition. Springer, New York.

Elliott, R. J., Aggoun, L., Moore, J. B., 1995. Hidden Markov models: estimation and control. Springer, New York.

Frederick, S., Loewenstein, G., O'donoghue, T., 2002. Time discounting and time preference: A critical review. Journal of Economic Literature, 351–401.

Garnaut, R., 2008. The Garnaut Climate Change Review: Final Report (2008). Cambridge University Press.

Garnaut, R., 2011. The Garnaut review 2011: Australia in the global response to climate change. Cambridge University Press.

Gollier, C., Treich, N., 2003. Decision-making under scientific uncertainty: the economics of the precautionary principle. Journal of Risk and Uncertainty 27 (1), 77–103.

Grenadier, S. R., Malenko, A., 2010. A Bayesian approach to real options: The case of distinguishing

between temporary and permanent shocks. The Journal of Finance 65 (5), 1949–1986.

Groom, B., Koundouri, P., Panopoulou, E., Pantelidis, T., 2007. Discounting the distant future: how much does model selection affect the certainty equivalent rate? Journal of Applied Econometrics 22 (3), 641–656.

Hartmann, D., Tank, A., Rusticucci, M., 2014. Observations: Atmosphere and surface. In: Stocker, T. F. (Ed.), Climate change 2013: the physical science basis: Working Group I contribution to the Fifth assessment report of the Intergovernmental Panel on Climate Change. Cambridge University Press, Ch. 2, pp. 159–254.

Hasson, A. E. A., Mills, G. A., Timbal, B., Walsh, K., 2009. Assessing the impact of climate change on extreme fire weather events over southeastern Australia. Climate Research 39 (2), 159–172.

Insurance Council of Australia, 2016. Historical disaster costs. http://www.insurancecouncil.com.au/assets/files/current%20and%20historical%20disaster%20statistics%20aug%2012.pdf.

Karatzas, I., Shreve, S., 1988. Brownian Motion and Stochastic Calculus. Springer, New York.

Karatzas, I., Zhao, X., 2001. Bayesian adaptive portfolio optimization. In: Jouini, E., Cvitanic, J., Musiela, M. (Eds.), Option Pricing, Interest Rates and Risk Management. Cambridge University Press, pp. 632–669.

Karp, L., Zhang, J., 2006. Regulation with anticipated learning about environmental damages. Journal of Environmental Economics and Management 51 (3), 259–279.

Keller, K., Bolker, B. M., Bradford, D. F., 2004. Uncertain climate thresholds and optimal economic growth. Journal of Environmental Economics and Management 48 (1), 723–741.

Kelly, D. L., Kolstad, C. D., 1999. Bayesian learning, growth, and pollution. Journal of Economic Dynamics and Control 23 (4), 491–518.

Kirshen, P., Knee, K., Ruth, M., 2008a. Climate change and coastal flooding in Metro Boston: impacts and adaptation strategies. Climatic Change 90 (4), 453–473.

Kirshen, P., Ruth, M., Anderson, W., 2008b. Interdependencies of urban climate change impacts and adaptation strategies: a case study of Metropolitan Boston USA. Climatic Change 86 (1-2), 105–122.

Klein, M., 2009. Comment on investment timing under incomplete information. Mathematics of Operations Research 34 (1), 249–254.

Koenker, R., Bassett, G., 1978. Regression quantiles. Econometrica, 33–50.

Ku-ring-gai Council, 2010. Climate change adaptation strategy. Tech. rep., Ku-ring-gai Council.

Lave, L. B., Apt, J., 2006. Planning for natural disasters in a stochastic world. Journal of Risk and Uncertainty 33 (1-2), 117–130.

Li, Y.-X., Tang, N., Jiang, X., In press. Bayesian approaches for analyzing earthquake catastrophic risk. Insurance: Mathematics and Economics.

Liptser, R., Shiryaev, A. N., 2001. Statistics of random Processes: I. general Theory. Springer, New York.

Lucas, C., 2010. On developing a historical fire weather data-set for Australia. Australian Meteorological and Oceanographic Journal 60 (1), 1.

Mathew, S., Trück, Henderson-Sellers, A., 2012. Kochi, India case study of climate adaptation to floods:

Ranking local government investment options. Global Environmental Change 22 (1), 308 – 319.

McFadden, D., 1973. Conditional logit analysis of qualitative choice behavior. Frontiers in Econometrics, 105–142.

Michael, J. A., 2007. Episodic flooding and the cost of sea-level rise. Ecological Economics 63 (1), 149–159.

Murphy, B. F., Timbal, B., 2008. A review of recent climate variability and climate change in southeastern Australia. International Journal of Climatology 28 (7), 859–879.

Newell, R. G., Pizer, W. A., 2003. Discounting the distant future: how much do uncertain rates increase valuations? Journal of Environmental Economics and Management 46 (1), 52–71.

Nordhaus, W. D., 2007. A review of the Stern review on the economics of climate change. Journal of Economic Literature, 686–702.

Oksendal, B., 2003. Stochastic Differential Equations: An Introduction with Applications, 6th Edition. Springer, New York.

Quigg, L., 1993. Empirical testing of real option-pricing models. The Journal of Finance 48 (2), 621–640.

Quiggin, J., 2008. Stern and his critics on discounting and climate change: an editorial essay. Climatic Change 89 (3), 195–205.

Rigby, R., Stasinopoulos, D., 2005. Generalized additive models for location, scale and shape. Journal of the Royal Statistical Society: Series C (Applied Statistics) 54 (3), 507–554.

Ryan, R., Lippman, S. A., 2003. Optimal exit from a project with noisy returns. Probability in the Engineering and Informational Sciences 17 (04), 435–458.

Schwartz, E. S., Trigeorgis, L., 2004. Real options and investment under uncertainty: classical readings and recent contributions. MIT press.

Shiryaev, A. N., 1978. Optimal stopping rules. Springer, New York.

Siu, T. K., 2016. A self-exciting threshold jump-diffusion model for option valuation. Insurance: Mathematics and Economics In Press.

Solomon, S., 2007. Climate change 2007 - the physical science basis: Working group I contribution to the fourth assessment report of the IPCC. Cambridge University Press.

Stern, N., 2007. The economics of climate change: the Stern review. Cambridge University Press.

Symes, D., Akbar, D., Gillen, M., Smith, P., 2009. Land-use mitigation strategies for storm surge risk in South East Queensland. Australian Geographer 40 (1), 121–136.

Tol, R. S., Yohe, G. W., 2009. The Stern review: a deconstruction. Energy Policy 37 (3), 1032–1040.

Truong, C., Trück, S., 2016. Its not now or never: Implications of investment timing and risk aversion on climate adaptation to extreme events. European Journal of Operational Research 253 (3), 856–868.

Van Aalst, M. K., 2006. The impacts of climate change on the risk of natural disasters. Disasters 30 (1), 5–18.

Waters, D., Watt, E., Marsalek, J., Anderson, B., 2003. Adaptation of a storm drainage system to accommodate increased rainfall resulting from climate change. Journal of Environmental Planning and Management 46 (5), 755–770.

Weitzman, M. L., 2009. On modeling and interpreting the economics of catastrophic climate change. The Review of Economics and Statistics 91 (1), 1–19.

West, J. J., Small, M. J., Dowlatabadi, H., 2001. Storms, investor decisions, and the economic impacts of sea level rise. Climatic Change 48 (2-3), 317–342.

Zhang, X., Elliott, R. J., Siu, T. K., 2012. A Bayesian approach for optimal reinsurance and investment in a diffusion model. Journal of Engineering Mathematics 76 (1), 195–206.

Zhu, T. J., Lund, J. R., Jenkins, M. W., Marques, G. F., Ritzema, R. S., 2007. Climate change, urbanization, and optimal long-term floodplain protection. Water Resources Research 43 (6).